Biophys Rev (2015) 7:183–190
DOI 10.1007/s12551-015-0164-8

REVIEW

Some (dis)assembly required: partial unfolding in the Par-6 allosteric switch

Dustin S. Whitney · Brian F. Volkman

Received: 1 November 2014 / Accepted: 12 January 2015 / Published online: 7 February 2015

Abstract Allostery is commonly described as a functional connection between two distant sites in a protein, where a binding event at one site alters affinity at the other. Here, we review the conformational dynamics that encode an allosteric switch in the PDZ domain of Par-6, which is a scaffold protein that organizes other proteins into a complex required to initiate and maintain cell polarity. NMR measurements revealed that the PDZ domain samples an evolutionarily conserved unfolding intermediate allowing rearrangement of two adjacent loop residues that control ligand binding affinity. Cdc42 binding to Par-6 creates a novel interface between the PDZ domain and the adjoining CRIB motif that stabilizes the high-affinity PDZ conformation. Thermodynamic and kinetic studies suggest that partial PDZ unfolding is an integral part of the Par-6 switching mechanism. The Par-6 CRIB-PDZ module illustrates two important structural aspects of protein evolution: the interface between adjacent domains in the same protein can give rise to allosteric regulation, and thermodynamic stability may be sacrificed to increase the sampling frequency of an unfolding intermediate required for conformational switching.

Keywords Protein folding · NMR · PDZ domain · Allostery · Conformational exchange · Cell polarity

This article is part of a Special Issue on 'The Role of Protein Dynamics in Allosteric Effects' edited by Gordon Roberts.

D. S. Whitney · B. F. Volkman (✉)
Department of Biochemistry, Medical College of Wiscsonsin, Milwaukee, WI 52336, USA
e-mail: bvolkman@mcw.edu

Present Address:
D. S. Whitney
Department of Biology, Massachusetts Institute of Technology, Cambridge, MA 02142, USA

Background

The establishment and maintenance of cell polarity is a key factor in a diverse array of biological contexts ranging from chemotactic cell migration to early embryonic development and the spatial organization of membranes and other tissues (Hung and Kemphues 1999; Johnston et al. 2011; Li et al. 2010; Lin et al. 2000; Nishimura et al. 2005; Welchman et al. 2007). Several modular PSD-95/Dlg/ZO-1 (PDZ) domain-containing protein complexes cooperate at the plasma membrane to initiate and maintain polarity by organizing the cytoskeleton and other cellular components to achieve the required spatial distribution and orientation (Wang and Margolis 2007; Bilder 2003). PDZ domains are small (~10-kDa) protein–protein interaction modules that typically bind a short sequence at the C-terminus of another protein. Most PDZ domains function as static binding modules within multi-domain (often multi-PDZ) scaffold proteins in combination with other types of protein interaction domains (Lee and Zheng 2010). However, an intriguing statistical analysis of coevolving residues in the PDZ family detected the potential for long-range energetic coupling (Lockless and Ranganathan 1999). Subsequent measurements of conformational dynamics have reinforced the notion that some PDZ domains could exhibit allosteric behavior (Fuentes et al. 2004; Petit et al. 2009; Zhang et al. 2010).

Partition defective 6 (Par-6/Pard-6) is a highly conserved central mediator of cell polarity that functions in concert with Par-3 and atypical protein kinase C (aPKC), and Cdc42 (Fig. 1a) (Lin et al. 2000; Garrard et al. 2003; Peterson et al. 2004; Watts et al. 1996). In addition to its PDZ domain, Par-6 contains an N-terminal Phox/Bem 1 (PB1) domain and a Cdc42/Rac Interaction Binding (CRIB) domain that adjoins the PDZ (Fig. 1b). The Par-6 PB1 domain associates with a homologous PB1 domain in aPKC, an indirectly regulated kinase that initiates downstream signaling. CRIB domains

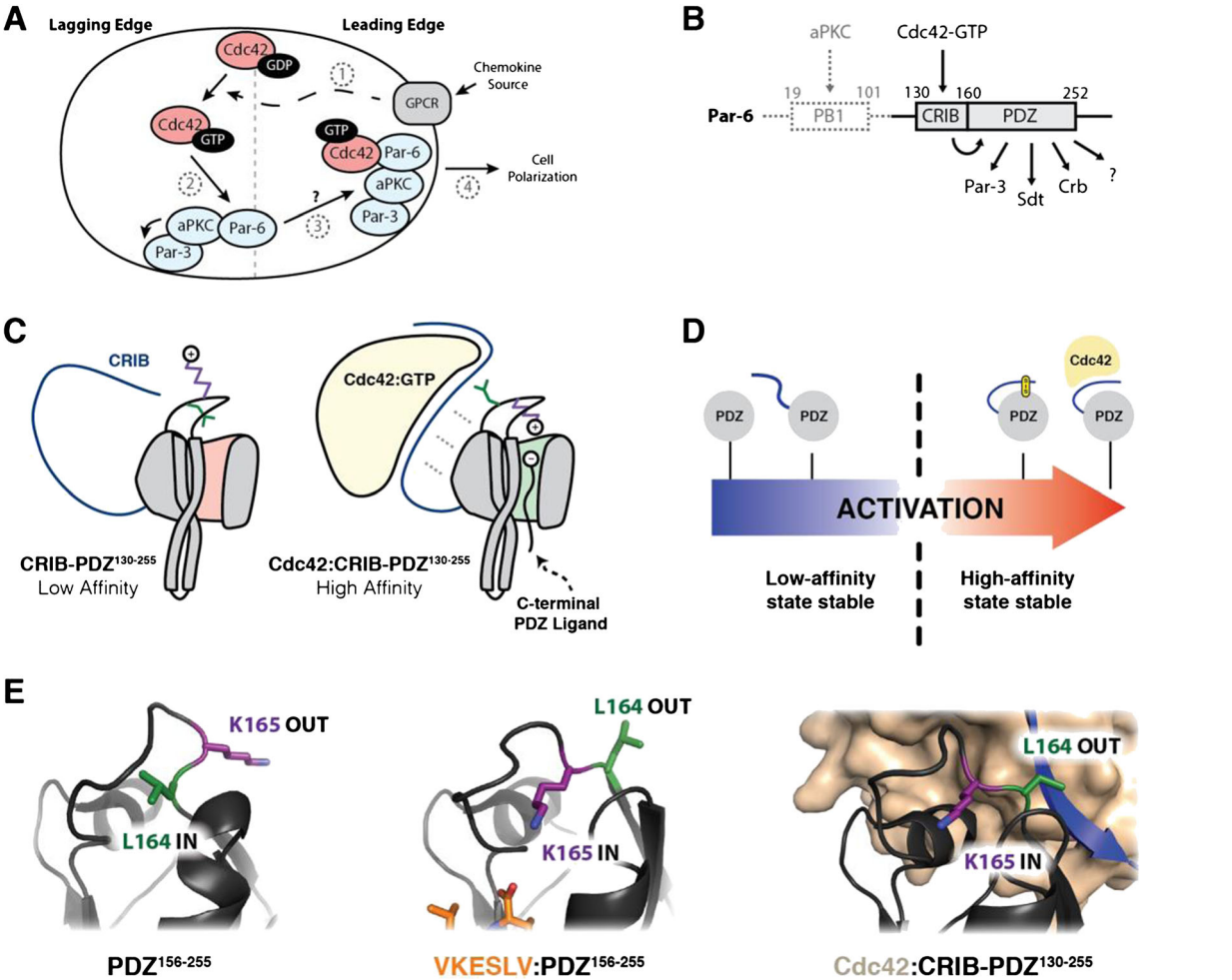

Fig. 1 Par-6 is a central mediator of cell polarity. **a** The Par polarity complex. **b**. Domains of Par-6 and interaction partners of each. **c** The L/K switching mechanism driven by Cdc42-GTP binding, allosterically shifting the Par-6 CRIB-PDZ$^{130–255}$ module into a high-affinity state. L164 is *dark green*, K165 *violet*. **d**. Continuum of binding activity for Par-6 constructs, reflecting their relative positions on the conformational equilibrium between low and high affinity states. **e**. Structural orientation of L/K switch residues in apo, VKESLV-bound, and Cdc42-bound states. L164 and K165 side chains are highlighted in *green* and *violet sticks*, respectively. *Orange sticks* indicate the VKESLV peptide and the Cdc42 surface is colored *tan*

consist of a short (~16 amino acids) consensus sequence motif that binds the Rho-family small GTPases Cdc42 or Rac1 by wrapping around the GTP-bound GTPase in an extended conformation (Abdul-Manan et al. 1999; Mott et al. 1999).

Cell polarization requires an input signal of GTP-loaded Cdc42. In contrast to other CRIB domains that bind GTPases in isolation (Prehoda et al. 2000; Lei et al. 2000; Kim et al. 2000), Cdc42 binds the Par-6 CRIB only if the adjacent PDZ domain is present (Garrard et al. 2003) (Fig. 1c). Upon Cdc42 binding, a portion of the flexible CRIB motif folds into a stable β-strand ('β_0') that pairs with the β_1 strand of the PDZ domain and forms a continuous nine-stranded intermolecular β-sheet with the GTPase, as illustrated by the crystal structure of Cdc42-GTP bound to the CRIB-PDZ module of Par-6 (Garrard et al. 2003). The functional consequence of Cdc42 binding is that the affinity of Par-6 for a model PDZ ligand peptide (VKESLV) is ~10 times higher than in the absence of Cdc42 (Peterson et al. 2004). Thus, the CRIB and PDZ domains of Par-6 (CRIB-PDZ$^{130–255}$) combine to form a GTPase-activated molecular switch that modulates Par-6 PDZ binding affinity (Peterson et al. 2004; Whitney et al. 2011) (Fig. 1c). Because the Cdc42 binding interface and the ligand binding cleft are separated by more than 10 Å, the discovery of this functional linkage was an unprecedented example of allostery in the PDZ domain family.

The Par-6 PDZ dipeptide switch regulates C-terminal ligand binding

The observation that Cdc42 enhances Par-6 binding to a C-terminal peptide ligand suggested that it induces a conformational change in the PDZ domain. However, comparisons of the NMR structure of the CRIB-PDZ module (CRIB-PDZ$^{130–}$

^{255}) (Peterson et al. 2004) and a crystal structure of the complex with Cdc42-GTP (Garrard et al. 2003) revealed only modest differences. Because a protein will populate all accessible conformations according to their relative free energies (Volkman et al. 1995; Palmer and Massi 2006; Palmer 2001; Hansen et al. 2008), we speculated that the PDZ domain might sample both the high- and low-affinity states even in the absence of Cdc42. Exchange broadening was observed in 2D ^{1}H-^{15}N HSQC spectra of CRIB-PDZ$^{130–255}$ for signals of the β_1 strand and other PDZ residues that contact the CRIB in the crystal structure of the complex with Cdc42-GTP (Whitney et al. 2011). Removal of the CRIB domain eliminated the broadening, which was ascribed to weak, transient CRIB-PDZ interactions that occur even in the absence of the GTPase. Importantly, ligand binding affinity as measured by fluorescence polarization using a rhodamine-labeled peptide (Whitney et al. 2011) was also diminished for the isolated PDZ domain relative to CRIB-PDZ$^{130–255}$ (Table 1). In addition, 2D HSQC spectra of PDZ$^{156–255}$, CRIB-PDZ$^{130–255}$ and the Cdc42:CRIB-PDZ$^{130–255}$ complex revealed a linear pattern of peaks(Whitney et al. 2011) that is a hallmark of fast exchange between two states (Volkman et al. 1995). We concluded that the PDZ domain exists in a conformational equilibrium that interconverts rapidly between low and high affinity states, and that weak interactions with the unstructured CRIB domain induce a modest population shift toward the high affinity conformation (Fig. 1d).

Since NMR and ligand binding studies indicated that PDZ$^{156–255}$ populates the low-affinity conformation to a greater degree than CRIB-PDZ$^{130–255}$ (Fig. 1d), we solved the NMR structure of the isolated PDZ domain (Whitney et al. 2011). Careful inspection of the PDZ$^{156–255}$ structure showed that it adopts a novel $\beta_{1–2}$ loop conformation in which the side chain of Lys 165 is solvent-exposed on the surface of the domain (the 'K165 out' configuration). In the other solved Par-6 structures, Lys 165 is buried in the hydrophobic core ('K165 in'), consistent with many other PDZ domains, where a conserved basic residue at this position places a positive charge at the base of the ligand binding cleft (Whitney et al. 2011; Li et al. 2006; Terrien et al. 2009; Tochio et al. 2000; Walma et al. 2002). The low-affinity K165 out configuration is stabilized in Par-6 by the concomitant burial of Leu 164 in the same location with the hydrophobic core (Fig. 1e). Because interconversion between the low- and high-affinity configurations essentially transposes the L164 and K165 side chains, we termed this structural element the 'L/K switch'.

As an independent verification of the L/K switch rearrangement, paramagnetic relaxation enhancement (PRE) experiments were used to compare the low-affinity ligand-free and high-affinity VKESLV-bound states of the CRIB-PDZ module (Whitney et al. 2013). Using a spin label (MTSL) conjugated to a cysteine in the PDZ $\beta_{1–2}$ loop (CRIB-PDZ^{L164C}), the location of this side chain was assessed by distance-dependent NMR signal relaxation (Gillespie and Shortle 1997). In the absence of a peptide ligand, selective PRE broadening of signals in the ^{1}H-^{15}N HSQC spectrum of CRIB-PDZ^{L164C} confirmed that the 164 side chain was buried in the PDZ core, corresponding to the 'K165 out' low affinity configuration observed in the PDZ$^{156–255}$ NMR structure (Fig. 1e) (Lockless and Ranganathan 1999). Addition of the VKESLV peptide completely changed the PRE profile such that NMR signals at the PDZ surface and in the CRIB domain were diminished by PRE, consistent with the high affinity 'K165 in. switch configuration seen in the Cdc42:CRIB-PDZ$^{130–255}$ and VKESLV:PDZ$^{156–255}$ X-ray crystal structures (Garrard et al. 2003; Peterson et al. 2004; Penkert et al. 2004) (Fig. 1e).

Table 1 Par-6 biochemical and dynamic data by construct in apo and VKESLV-bound states

	K_d^{VKESLV}	ΔG_{unf}	apo		+ VKESLV	
			R_{ex}	k_{ex}	R_{ex}	k_{ex}
PDZ$^{156–255}$	72±5 μM	3.2±0.3 kcal/mol	+++	1600 s^{-1}	–	n/a
CRIB-PDZ$^{130–255}$	54±5 μM	2.8±0.4 kcal/mol	+++	1600 s^{-1}	+++	1800 s^{-1}
CRIB-PDZ$^{Q144C/L164C}$	13±2 μM	5.1±0.1 kcal/mol	+++	1600 s^{-1}	–	n/a

Effect of CRIB removal and disulfide linking on VKESLV binding, ΔG_{unfold}, R_{ex} coverage of the PDZ domain, and globally fitted k_{ex} values for apo and VKESLV-bound constructs. Biochemical experiments were conducted at 25 °C, and CPMG-based dynamics experiments were conducted at 15 and 25 °C

Stable association of the CRIB domain is sufficient to activate the PDZ switch

Par-6 PDZ ligand binding affinity is slightly reduced by removal of the CRIB domain, presumably due to an increase the relative population of the low affinity conformation. To test the hypothesis that formation of the interdomain CRIB-PDZ interface is sufficient to activate the L/K switch, we designed a disulfide-stabilized CRIB-PDZ$^{130–255}$ variant. Cysteine substitutions in the CRIB (Q144C) and the $\beta_{1–2}$ loop (L164C) (CRIB-PDZ$^{Q144C/L164C}$) readily formed a disulfide designed to position the CRIB in a conformation that mimics the Cdc42-bound X-ray structure (Garrard et al. 2003). Because the side chain of position 164 is engaged in a disulfide with the CRIB, it can no longer occupy the PDZ hydrophobic core and the low-affinity L/K switch conformation is no longer accessible. CRIB-PDZ$^{Q144C/L164C}$ bound to VKESLV nearly as tightly as Cdc42:CRIB-PDZ$^{130–255}$, a 4.3-fold improvement over CRIB-PDZ$^{130–255}$ (Fig. 1d) (Whitney et al. 2011). The NMR solution structure of CRIB-PDZ$^{Q144C/L164C}$ revealed

that the disulfide-tethered CRIB residues adopt a similar conformation to the CRIB in the Cdc42:CRIB-PDZ$^{130–255}$ complex, and that Lys 165 was indeed inserted into the PDZ core, matching both the conserved orientation of the conserved basic side chain in PDZ family domains and the high-affinity state seen in previous crystal structures of Par-6 (Whitney et al. 2011).

The dipeptide switch obscures a larger domain transition

Remodeling of the $\beta_{1–2}$ loop in Par-6 appeared to be a simple case of localized conformational exchange in a protein, where a two-residue isomerization event (the L/K switch) in a flexible loop drives affinity switching (Fig. 1c). Ligand-free CRIB-PDZ$^{130–255}$ demonstrated NMR exchange broadening near the CRIB:PDZ interface, diagnostic of motions on the μs-ms timescale that we attributed to transient contacts between the flexible CRIB and the PDZ domain (Whitney et al. 2011). We speculated that the intrinsic rate of L/K switch interconversion would be similar. CPMG-based R_2 dispersion experiments are useful for characterizing in a site-specific manner the kinetics of motions that cause broadening on the μs-ms timescale (Palmer and Massi 2006; Hansen et al. 2008). We employed these methods to quantify the intrinsic rate of L/K switching in the Par-6 CRIB-PDZ module, expecting that enhanced ^{15}N R_2 relaxation arising from conformational exchange (R_{ex}) would be localized to the immediate vicinity (e.g. residues of the $\beta_{1–2}$ loop). Instead, R_{ex} was evident throughout apo CRIB-PDZ$^{130–255}$ (Fig. 2a) (Whitney et al. 2013), indicating that nearly the entire PDZ structure participates in or reports on a conformational rearrangement.

In the analysis of R_2 dispersion data, residues exhibiting similar exchange rates are grouped to define regions of the protein that may undergo a concerted conformational rearrangement (O'Connor and Kovrigin 2008; Kovrigin et al. 2006). Careful inspection of individual exchange rate constants (k_{ex}) yielded a predominant set of residues that were fitted to a single k_{ex} of ~1600 s^{-1} (Table 1) (Whitney et al. 2013). Strikingly, comparable sets of residues in both PDZ$^{156–255}$ and CRIB-PDZ$^{Q144C/L164C}$ were globally fitted to similar k_{ex} values, suggesting that: (1) a large portion of the PDZ domain undergoes a sub-millisecond conformational rearrangement; (2) the rate of intrinsic motions is independent of the relative stability of the high- and low-affinity states; and (3) because L/K switch flipping is effectively eliminated by the disulfide link of CRIB-PDZ$^{Q144C/L164C}$ but R_{ex} persists, the rearrangement is intrinsic to the PDZ domain rather than being driven by the L/K switch itself (Whitney et al. 2013).

Peptide binding quenches some internal motions in the PDZ

Allosteric mechanisms require at minimum two functional sites. The first is where input signal is received and the second is a distal functional site that is altered upon receipt of the input signal (e.g., a binding event). It follows that, since the input into the first site alters binding affinity at the second site, an allosteric protein will achieve the lowest-energy configuration when the input signal is present and the second site is occupied by its ligand.

Our measurements thus far manipulated only the input site (Cdc42 binding interface), so we studied the internal μs-ms dynamic motions of Par-6 upon C-terminal ligand binding

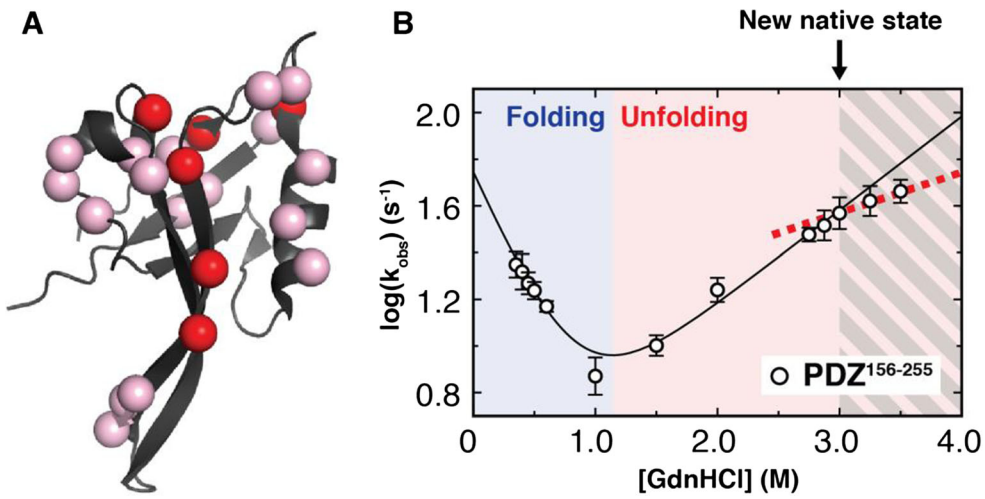

Fig. 2 Par-6 dynamics are linked to a partial unfolding process. **a** Residues reporting R_{ex} for PDZ$^{156–255}$ and CRIB-PDZ$^{130–255}$ (*pink* and *red spheres*). *Red spheres* are also globally fitted for exchange rate constants (k_{ex}). **b** Chevron rollover (*gray hatched area*) in the unfolding arm of stopped-flow fluorescence measurements of GuHCl-induced folding/unfolding of PDZ$^{156–255}$. The presence of an unfolding intermediate is revealed by a transition in the unfolding arm to a shallower slope (*red dashed line*) at higher denaturant concentrations

(Whitney et al. 2013). PDZ$^{156–255}$, CRIB-PDZ$^{130–255}$, and CRIB-PDZ$^{Q144C/L164C}$ were bound to saturating concentrations of the C-terminal ligand VKESLV and their internal dynamic motions were individually and globally fitted when appropriate. VKESLV:PDZ$^{156–255}$ exhibited reduced R_{ex} across the PDZ domain (Table 1). Where over 30 residues had significant R_{ex} in apo PDZ$^{156–255}$, only 9 retained dispersions, all of which appeared to be uncorrelated. Similarly, VKESLV:CRIB-PDZ$^{Q144C/L164C}$ reported a similar but stronger reduction of residues reporting R_2 dispersions (Table 1). Only two residues retained significant R_{ex} when VKESLV was bound, indicating that ligand binding reduces internal dynamic motions within the Par-6 PDZ when CRIB residues were either truncated or spatially restricted by disulfide link.

Strikingly, we observed a divergent dynamic profile for VKESLV:CRIB-PDZ$^{130–255}$. The natural protein, with untethered CRIB residues present, continued to report domain-wide R_{ex}. Though the distribution of R_2 dispersions was altered somewhat, many of the same residues were globally fitted for apo CRIB-PDZ$^{130–255}$ and VKESLV:CRIB-PDZ$^{130–255}$, and motions were fitted to a similar k_{ex} of ~1800 s^{-1} (Table 1). This suggested that dynamic fluctuations of the untethered CRIB influence the PDZ domain even when a peptide occupies the ligand binding cleft. Furthermore, the similarity of exchange rate constants for VKESLV:CRIB-PDZ$^{130–255}$ motions and apo PDZ$^{156–255}$ suggests that CRIB motions are frequency-matched to the intrinsic domain-wide PDZ rearrangement.

CRIB-mediated Par-6 PDZ destabilization drives conformational exchange

Conformational exchange occurs in proteins that possess at least one kinetically accessible alternative conformation similar in folding energy to the native state. Alternative state(s) are populated at a ratio determined by the difference in free energy and accessed at rates determined by the height of the energetic unfolding barrier between them. Destabilization of the predominant native conformation shifts the population toward one or more alternative/non-native states. Whereas an infinitely stable protein would adopt only one conformation and display no dynamic motions, large excursions from the average conformation may indicate that the native state is only marginally stable.

We speculated that persistent μs–ms dynamic motions in the VKESLV:CRIB-PDZ$^{130–255}$ complex might result from a PDZ-destabilizing effect of the untethered CRIB domain. Interestingly, the isolated PDZ domain is only moderately stable, as measured using fluorescence intensity of the single tyrosine residue (Y175) to monitor guanidine HCl-induced equilibrium unfolding (ΔG_{unf}=3.2 kcal/mol) (Whitney et al. 2013). Moreover, the linked CRIB domain destabilizes the PDZ by 0.4 kcal/mol (Table 1), suggesting that the dynamic motions reported might reflect an unfolding transition (Whitney et al. 2013). In comparison, CRIB-PDZ$^{Q144C/L164C}$ is significantly more stable (ΔG_{unf}=5.1 kcal/mol) and VKESLV binding quenches virtually all of the R_{ex} observed in the other VKESLV complexes. For a protein that exhibits two-state folding, the occupancy of the unfolded state at a particular temperature may be estimated from the free energy of folding. For instance, at 25 °C, a protein with ΔG_{unf}=5 kcal/mol is ~0.02 % unfolded. In contrast, the Par-6 CRIB-PDZ$^{130–255}$ module (ΔG_{unf}=2.7 kcal/mol) would be predicted to consist of ~99 % folded and ~1 % unfolded protein at equilibrium. Frequent (e.g., ms–μs) sampling of a partially or globally unfolded conformation would necessarily produce conformational exchange broadening like the pervasive R_{ex} observed for the Par-6 PDZ domain.

Evolutionarily conserved partial unfolding permits an allosteric mechanism

The persistence of dynamic CRIB-driven motions in VKESLV:CRIB-PDZ$^{130–255}$ also lowered protein stability in the PDZ domain, so we tested whether a folding transition was responsible for detected domain-wide dynamic motions using single-jump stop-flow measurements of Y175 fluorescence. Extrapolation of kinetic folding and unfolding rates from the resultant chevron plot revealed that the sum of global folding and unfolding rates was >10-fold slower than the measured k_{ex} from CPMG-based R_2 dispersion measurements (Whitney et al. 2013), thus it was unlikely these motions reported on the same process. During data analysis, however, we detected chevron rollover in the unfolding arm of the kinetic experiments on CRIB-PDZ$^{130–255}$ and PDZ$^{156–255}$ at higher guanidine HCl concentrations (Fig. 2b). Chevron rollover is a deviation from linearity in one "arm" of a chevron plot: it reflects a change in the low energy state of the protein at higher denaturant concentration. Because partially unfolded states can become more stable than the native conformation in the presence of high denaturant levels, rollover is commonly interpreted as evidence for one or more on-pathway unfolding intermediates (Chi et al. 2007, 2009; Feng et al. 2005a).

Subsequent NMR ^{1}H-^{2}D solvent exchange experiments supported this observation (Whitney et al. 2013). Briefly, ^{15}N HSQC peak intensities are recorded serially following resuspension of a dried, protonated protein powder in 100 % D_2O containing various concentrations of guanidine HCl; their decays are fitted for amide exchange rates and plotted versus the concentration of denaturant. Backbone amide exchange rates remain constant at lower denaturant levels (Bai et al. 1995) for residues that participate only in global unfolding. In contrast, amides that sense or participate in partial unfolding transitions exhibit a negative linear dependence

of ^{1}H-^{2}D exchange rate on denaturant concentrations below those sufficient to drive global unfolding (Feng et al. 2005b; Bai et al. 2007). A cluster of residues reporting partial unfolding corroborated the existence of a folding intermediate in the Par-6 PDZ and further indicated that the detected folding transition likely involved the PDZ $\beta_{2–3}$ finger (Whitney et al. 2013). This was particularly interesting because CPMG-based R_2 dispersion analysis indicated that $\beta_{2–3}$ finger residues participated in the internal dynamics of the PDZ in each of the constructs analyzed by NMR (Fig. 2a) (Whitney et al. 2013).

Other groups have previously detailed an evolutionarily conserved partial folding intermediate across several archetypal PDZ domains (Chi et al. 2007; Feng et al. 2005b; Jemth and Gianni 2007; Ivarsson et al. 2007; Gianni et al. 2007). Despite a 13 % sequence identity between them, each populates an on-pathway folding intermediate, including all three PDZ domains from PTP-BL, PDZ3 from PSD-95, PDZ2 from SAP97, and the nNOS PDZ (Chi et al. 2007, 2009). The transition state position along the folding reaction was similar for each PDZ, suggesting a conserved folding mechanism that spans the domain family. Similar to our data, these studies detected chevron rollover in the unfolding arm (Fig. 2b). Furthermore, Φ-value analysis suggested that undocking of the $\beta_{2–3}$ finger from the PDZ core was the likely second transition step between the folding intermediate and the native state(Gianni et al. 2007).

Close inspection of native (zero denaturant) ^{1}H-^{2}D exchange rates for individual residues can indicate which structural regions of a domain are most stably folded (Bai et al. 1995). We compared the most solvent-protected amides in native ^{1}H-^{2}D exchange experiments to those PDZ residues exhibiting no R_2 dispersion (R_{ex}=0) in each construct(Whitney et al. 2013). The common population, residues most stably folded and insensate to any dynamic fluctuations, defined a portion of the PDZ core furthest from the $\beta_{2–3}$ finger. Conversely, residues exhibiting significant R_{ex} and lower ^{1}H-^{2}D exchange protection factors indicative of partial unfolding are located within or proximal to the $\beta_{2–3}$ finger (Whitney et al. 2013). Taken together, the results suggest that partial unfolding in the Par-6 PDZ detected by kinetic measurements corresponds to detachment of the $\beta_{2–3}$ finger from the rest of the PDZ fold, consistent with observations of a folding intermediate in other PDZ domains (Fig. 3a).

One dynamic process permits another

Par-6 allostery is a tale of at least two types of internal motion: unfolding and isomerization. A partial unfolding transition common to many or all PDZ domains was observed in Par-6 (Fig. 2b). Instability of the Par-6 PDZ domain ($\Delta G_{unf} \approx 3$ kcal/mol), relative to other PDZ domains(Chi et al. 2007; Feng et al. 2005b), permits increased access to partially unfolded states. Weak interdomain contacts with the N-terminally adjacent CRIB domain further increase PDZ domain access to an unfolded state (Table 1) (Whitney et al. 2013). Ligand binding to the protein stabilizes the PDZ such that the unfolding transition is silenced and its μs-ms motions are no longer detected as ^{15}N R_{ex}.

Conformational isomerization—two-site exchange of the L164 and K165 side chains—is dependent on the unfolding transition. The L/K switch in the $\beta_{1–2}$ loop determines the affinity state of C-terminal PDZ ligand binding, but it likely cannot "flip" without the extra flexibility provided by a partially unfolded intermediate. On the other hand, domain-wide motion in the disulfide-stabilized CRIB-PDZ$^{Q144C/L164C}$ is similar to the other Par-6 constructs despite chemical restriction of the L/K switch to a single configuration. Thus, switch motions can be restricted by enhanced PDZ thermodynamic stability that limits access to the partially unfolded intermediate, but the unfolding transition is intrinsic to the

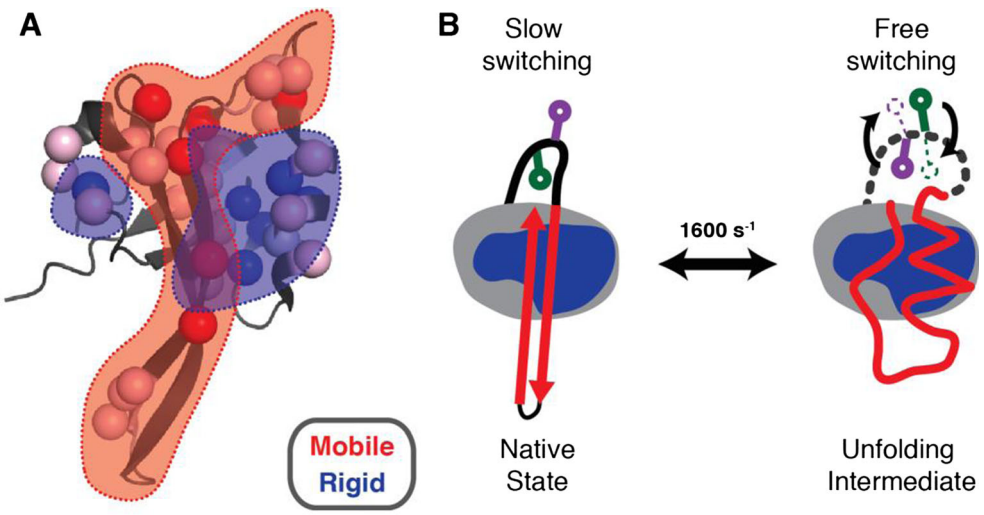

Fig. 3 A model for partial unfolding in the Par-6 PDZ. **a**. Distinct regions of dynamic motion and stability are shown as *red* and *blue* on the ribbon $PDZ^{156–255}$ structure, respectively. **b** Stylized representation of $\beta_{2–3}$ finger undocking from the PDZ core. In the proposed model, L/K switch interconversion occurs freely in the unfolding intermediate. L164 position is *dark green*, K165 position indicated by *violet*

PDZ domain and possibly conserved throughout the family (Fig. 3b).

Evolved instability for allosteric regulation in Par-6

Proteins evolve through preservation of amino acid sequence changes that yield a new or better function. Mutations that diminish protein stability are said to reduce 'fitness' by reducing the concentration of folded, functional molecules (Tokuriki and Tawfik 2009). In this view, when protein fitness is compromised ($\Delta G_{unfold} \leq 3$ kcal/mol), the ultimate fate of the destabilizing mutation is usually elimination. When linked to the CRIB domain, the Par-6 PDZ is thermodynamically unstable ($\Delta G_{unf} = 2.7$ kcal/mol) relative to other PDZ domains, and the higher fraction of unfolded molecules could be viewed as a compromise of fitness.

However, a more stable Par-6 CRIB-PDZ module would access the unfolded state less frequently. Our results suggest that access to the partially unfolded state is critical for interconversion of the L/K switch and that this enables GTPase regulation of PDZ binding affinity. Conversely, if ΔG_{unfold} was further reduced to 2 kcal/mol, ~3.5 % of the protein would be globally unfolded at 25 ° C, more than tripling the unfolded conformation and exposing Par-6 to increased degradation or aggregation. Thus, marginal thermodynamic stability of the CRIB-PDZ module appears to be optimized for its specialized function as a molecular switch, and Par-6 is the first PDZ protein shown to utilize a conserved unfolding intermediate in a functional role.

Conclusions

Activation of Cdc42 by the exchange of GDP for GTP initiates key signal transduction pathways leading to cell polarization, among which is an allosteric change in the Par-6 PDZ binding affinity. In this review, we have summarized the unusual mechanism by which Cdc42 alters the affinity of Par-6 PDZ for C-terminal ligands. However, Par-6 is among a small number of PDZ proteins that bind to a non-canonical internal sequence (non-carboxyl terminal) ligand. Its interaction with the protein Pals1 has been characterized in detail, including the crystal structure of a PDZ:Pals1 complex (Penkert et al. 2004). Strikingly, the binding affinity of the Par6:Pals1 interaction is unaffected by Cdc42 (Peterson et al. 2004). Thus, allosteric PDZ affinity switching in Par-6 is context-dependent, applying only to C-terminal ligands. The mechanism by which Par-6 is subject to selectively regulated ligand binding remains a topic of interest and ongoing investigation.

Coupling of the GTPase-stabilized CRIB-PDZ interface to the PDZ ligand binding pocket is a prototypical example of interdomain allostery contributing to the formation of a novel regulatory mechanism (Lee et al. 2008). We now perceive that the Par-6 conformational switch mechanism employs an unfolding intermediate that is accessible because the PDZ domain is less thermodynamically stable than most PDZ domains. Weak interactions with the attached CRIB domain further destabilize the native PDZ fold while slightly enhancing ligand binding affinity. Cdc42 binding stabilizes the CRIB-PDZ interface and the high-affinity state of the dipeptide switch. We speculate that functional unfolding transitions like the one employed by Par-6 are more common than we currently realize, given the challenges of measuring internal dynamics of proteins. The potential for native-state unfolding and other types of protein dynamics to increase fitness may lead to refinements of the current paradigm for the evolution of protein structure and function.

Compliance with ethical standards

Funding This work was supported by NIH research grants R01 AI058072, R56 AI013225, and S10 RR024665.

Conflict of interest Dustin Whitney declares that he has no conflict of interest.

Brian Volkman declares that he has no conflict of interest.

Ethical approval This article does not contain any studies with human participants or animals performed by any of the authors.

References

Abdul-Manan N, Aghazadeh B, Liu GA, Majumdar A, Ouerfelli O, Siminovitch KA, Rosen MK (1999) Structure of Cdc42 in complex with the GTPase-binding domain of the 'Wiskott-Aldrich syndrome' protein. Nature 399:379–383

Bai Y, Sosnick TR, Mayne L, Englander SW (1995) Protein folding intermediates: native-state hydrogen exchange. Science 269:192–197

Bai Y, Feng H, Zhou Z (2007) Population and structure determination of hidden folding intermediates by native-state hydrogen exchange-directed protein engineering and nuclear magnetic resonance. Methods Mol Biol 350:69–81

Bilder D (2003) PDZ domain polarity complexes. Curr Biol 13:R661–R662

Chi CN, Gianni S, Calosci N, Travaglini-Allocatelli C, Engstrom K, Jemth P (2007) A conserved folding mechanism for PDZ domains. FEBS Lett 581:1109–1113

Chi CN, Bach A, Engstrom A, Wang H, Stromgaard K, Gianni S, Jemth P (2009) A sequential binding mechanism in a PDZ domain. Biochemistry 48:7089–7097

Feng H, Zhou Z, Bai Y (2005a) A protein folding pathway with multiple folding intermediates at atomic resolution. Proc Natl Acad Sci U S A 102:5026–5031

Feng H, Vu ND, Bai Y (2005b) Detection of a hidden folding intermediate of the third domain of PDZ. J Mol Biol 346:345–353

Fuentes EJ, Der CJ, Lee AL (2004) Ligand-dependent dynamics and intramolecular signaling in a PDZ domain. J Mol Biol 335:1105–1115

Garrard SM, Capaldo CT, Gao L, Rosen MK, Macara IG, Tomchick DR (2003) Structure of Cdc42 in a complex with the GTPase-binding domain of the cell polarity protein, Par6. EMBO J 22:1125–1133

Gianni S, Geierhaas CD, Calosci N, Jemth P, Vuister GW, Travaglini-Allocatelli C, Vendruscolo M, Brunori M (2007) A PDZ domain recapitulates a unifying mechanism for protein folding. Proc Natl Acad Sci U S A 104:128–133

Gillespie JR, Shortle D (1997) Characterization of long-range structure in the denatured state of staphylococcal nuclease. II. Distance restraints from paramagnetic relaxation and calculation of an ensemble of structures. J Mol Biol 268:170–184

Hansen DF, Vallurupalli P, Lundstrom P, Neudecker P, Kay LE (2008) Probing chemical shifts of invisible states of proteins with relaxation dispersion NMR spectroscopy: how well can we do? J Am Chem Soc 130:2667–2675

Hung TJ, Kemphues KJ (1999) PAR-6 is a conserved PDZ domain-containing protein that colocalizes with PAR-3 in Caenorhabditis elegans embryos. Development 126:127–135

Ivarsson Y, Travaglini-Allocatelli C, Jemth P, Malatesta F, Brunori M, Gianni S (2007) An on-pathway intermediate in the folding of a PDZ domain. J Biol Chem 282:8568–8572

Jemth P, Gianni S (2007) PDZ domains: folding and binding. Biochemistry 46:8701–8708

Johnston CA, Whitney DS, Volkman BF, Doe CQ, Prehoda KE (2011) Conversion of the enzyme guanylate kinase into a mitotic-spindle orienting protein by a single mutation that inhibits GMP-induced closing. Proc Natl Acad Sci U S A 108:E973–E978

Kim AS, Kakalis LT, Abdul-Manan N, Liu GA, Rosen MK (2000) Autoinhibition and activation mechanisms of the Wiskott-Aldrich syndrome protein. Nature 404:151–158

Kovrigin EL, Kempf JG, Grey MJ, Loria JP (2006) Faithful estimation of dynamics parameters from CPMG relaxation dispersion measurements. J Magn Reson 180:93–104

Lee HJ, Zheng JJ (2010) PDZ domains and their binding partners: structure, specificity, and modification. Cell Commun Signal 8:8

Lee J, Natarajan M, Nashine VC, Socolich M, Vo T, Russ WP, Benkovic SJ, Ranganathan R (2008) Surface sites for engineering allosteric control in proteins. Science 322:438–442

Lei M, Lu W, Meng W, Parrini MC, Eck MJ, Mayer BJ, Harrison SC (2000) Structure of PAK1 in an autoinhibited conformation reveals a multistage activation switch. Cell 102:387–397

Li X, Zhang J, Cao Z, Wu J, Shi Y (2006) Solution structure of GOPC PDZ domain and its interaction with the C-terminal motif of neuroligin. Protein Sci Publ Protein Soc 15:2149–2158

Li J, Kim H, Aceto DG, Hung J, Aono S, Kemphues KJ (2010) Binding to PKC-3, but not to PAR-3 or to a conventional PDZ domain ligand, is required for PAR-6 function in C. elegans. Dev Biol 340:88–98

Lin D, Edwards AS, Fawcett JP, Mbamalu G, Scott JD, Pawson T (2000) A mammalian PAR-3-PAR-6 complex implicated in Cdc42/Rac1 and aPKC signalling and cell polarity. Nat Cell Biol 2:540–547

Lockless SW, Ranganathan R (1999) Evolutionarily conserved pathways of energetic connectivity in protein families. Science 286:295–299

Mott HR, Owen D, Nietlispach D, Lowe PN, Manser E, Lim L, Laue ED (1999) Structure of the small G protein Cdc42 bound to the GTPase-binding domain of ACK. Nature 399:384–388

Nishimura T, Yamaguchi T, Kato K, Yoshizawa M, Nabeshima Y, Ohno S, Hoshino M, Kaibuchi K (2005) PAR-6-PAR-3 mediates Cdc42-induced Rac activation through the Rac GEFs STEF/Tiam1. Nat Cell Biol 7:270–277

O'Connor C, Kovrigin EL (2008) Global conformational dynamics in ras. Biochemistry 47:10244–10246

Palmer AG 3rd (2001) Nmr probes of molecular dynamics: overview and comparison with other techniques. Annu Rev Biophys Biomol Struct 30:129–155

Palmer AG 3rd, Massi F (2006) Characterization of the dynamics of biomacromolecules using rotating-frame spin relaxation NMR spectroscopy. Chem Rev 106:1700–1719

Penkert RR, DiVittorio HM, Prehoda KE (2004) Internal recognition through PDZ domain plasticity in the Par-6-Pals1 complex. Nat Struct Mol Biol 11:1122–1127

Peterson FC, Penkert RR, Volkman BF, Prehoda KE (2004) Cdc42 regulates the Par-6 PDZ domain through an allosteric CRIB-PDZ transition. Mol Cell 13:665–676

Petit CM, Zhang J, Sapienza PJ, Fuentes EJ, Lee AL (2009) Hidden dynamic allostery in a PDZ domain. Proc Natl Acad Sci U S A 106:18249–18254

Prehoda KE, Scott JA, Mullins RD, Lim WA (2000) Integration of multiple signals through cooperative regulation of the N-WASP-Arp2/3 complex. Science 290:801–806

Terrien E, Simenel C, Prehaud C, Buc H, Delepierre M, Lafon M, Wolff N (2009) 1H, 13C and 15N resonance assignments of the PDZ of microtubule-associated serine/threonine kinase 205 (MAST205) in complex with the C-terminal motif from the rabies virus glycoprotein. Biomol NMR Assignments 3:45–48

Tochio H, Mok YK, Zhang Q, Kan HM, Bredt DS, Zhang M (2000) Formation of nNOS/PSD-95 PDZ dimer requires a preformed beta-finger structure from the nNOS PDZ domain. J Mol Biol 303: 359–370

Tokuriki N, Tawfik DS (2009) Stability effects of mutations and protein evolvability. Curr Opin Struct Biol 19:596–604

Volkman BF, Nohaile MJ, Amy NK, Kustu S, Wemmer DE (1995) Three-dimensional solution structure of the N-terminal receiver domain of NTRC. Biochemistry 34:1413–1424

Walma T, Spronk CA, Tessari M, Aelen J, Schepens J, Hendriks W, Vuister GW (2002) Structure, dynamics and binding characteristics of the second PDZ domain of PTP-BL. J Mol Biol 316:1101–1110

Wang Q, Margolis B (2007) Apical junctional complexes and cell polarity. Kidney Int 72:1448–1458

Watts JL, Etemad-Moghadam B, Guo S, Boyd L, Draper BW, Mello CC, Priess JR, Kemphues KJ (1996) par-6, a gene involved in the establishment of asymmetry in early C. elegans embryos, mediates the asymmetric localization of PAR-3. Development 122:3133–3140

Welchman DP, Mathies LD, Ahringer J (2007) Similar requirements for CDC-42 and the PAR-3/PAR-6/PKC-3 complex in diverse cell types. Dev Biol 305:347–357

Whitney DS, Peterson FC, Volkman BF (2011) A conformational switch in the CRIB-PDZ module of Par-6. Structure 19:1711–1722

Whitney DS, Peterson FC, Kovrigin EL, Volkman BF (2013) Allosteric activation of the Par-6 PDZ via a partial unfolding transition. J Am Chem Soc 135:9377–9383

Zhang J, Sapienza PJ, Ke H, Chang A, Hengel SR, Wang H, Phillips GN, Lee AL (2010) Crystallographic and nuclear magnetic resonance evaluation of the impact of peptide binding to the second PDZ domain of protein tyrosine phosphatase 1E. Biochemistry 49:9280–9291